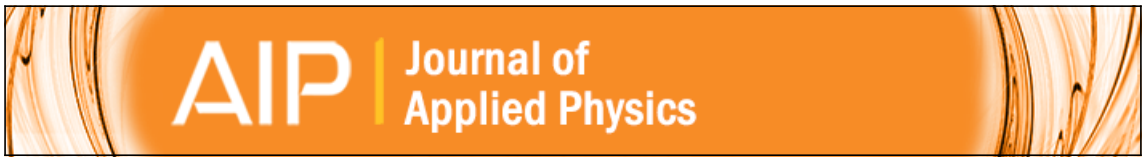

Compositional evolution and magnetic properties of nanocrystalline Fe73.5Cu1Nb3Si13.5B9

M. Knobel, R. Sato Turtelli, and H. R. Rechenberg

Citation: Journal of Applied Physics **71**, 6008 (1992); doi: 10.1063/1.350455

View online: http://dx.doi.org/10.1063/1.350455

View Table of Contents: http://scitation.aip.org/content/aip/journal/jap/71/12?ver=pdfcov

Published by the AIP Publishing

Compositional evolution and magnetic properties of nanocrystalline $Fe_{73.5}Cu_1Nb_3Si_{13.5}B_9$

M. Knobel and R. Sato Turtelli
Instituto de Fisica Gleb Wataghin, UNICAMP, Caixa Postal 6165, 13 081 Campinas, São Paulo, Brazil

H. R. Rechenberg
Instituto de Fisica, Universidade de São Paulo, Caixa Postal 20516, 01498 São Paulo, Brazil

(Received 13 January 1992; accepted for publication 4 March 1992)

Melt-spun FeCuNbSiB ribbons were annealed at 540–550 °C for various times ($\leqslant$1 h). The development of a nanocrystalline structure was investigated by means of Mössbauer spectroscopy. From measured hyperfine fields and intensities the crystalline phase was inferred to be pure $Fe_{1-x}Si_x$, with $x=0.18$ after 1 h annealing. The residual amorphous volume fraction was determined to be $\simeq$50%. With help of these results it has been possible to evaluate the amorphous contribution to magnetostriction in the nanocrystalline state. The development of a nanocrystalline structure was found to play a role in the main mechanisms of magnetic disaccommodation.

I. INTRODUCTION

The so-called nanocrystalline materials are solids composed mainly of two structural phases, i.e., nanometer-sized crystallites (10–20 nm) randomly distributed in an amorphous matrix.[1] Most recently, special attention has been given to nanocrystalline material obtained by controlled crystallization of metal-metalloid amorphous ribbons. In particular, the devitrified glassy $Fe_{73.5}Cu_1Nb_3Si_{13.5}B_9$ has been researched as it exhibits a combination of remarkable soft magnetic properties.[2–4] These superior soft magnetic properties are due to the magnetocrystalline anisotropy of the α-FeSi grains randomly averaged out due to exchange interaction between grains, since the latter become smaller than the exchange length. In addition, the high Si content of the crystalline phase simultaneously leads to very low saturation magnetostriction.[3,5]

After a proper annealing (typically 1 h at 520–560 °C), the material presents an ultrafine grain structure (around 10 nm) of bcc-Fe-Si embedded in a residual amorphous phase. The formation of the nanocrystalline structure is ascribed to the combined addition of Cu and Nb (which are not soluble in α-Fe) in the glassy Fe-Si-B. While Cu enhances the nucleation rate of α-Fe grains, Nb hinders the grain growth due to its higher thermal stability.[6,7]

Several studies concerning the development of the nanocrystalline phase have been reported. However, the kinetics of the crystallization process, as well as the composition and volume fractions of the phases resulting from the heat treatment, are still not fully understood. Another important point is the role played by boron in the crystallization process. Besides the controversy over the presence of interstitial B in the α-Fe-Si lattice, it is important to know if Fe-B compounds are formed upon annealing. Compounds of this sort will lead to deterioration of the soft magnetic properties owing to their larger magnetocrystalline anisotropy.[8]

In this work, a study of the development of the nanocrystalline phase in the $Fe_{73.5}Cu_1Nb_3Si_{13.5}B_9$ alloy using Mössbauer spectroscopy is presented. When properly analyzed, Mössbauer spectra can yield information not easily obtained by other methods. Heat treatments with fixed temperature and different times were performed. The results show the compositional evolution of the constituent phases, reflecting the diffusion processes that occur during the formation of the nanocrystalline state. The amorphous and crystalline volume fractions have also been determined. Combining these data with magnetostriction and disaccommodation results, one can gain insight into the basic mechanisms responsible for the very low saturation magnetostriction and nearly null magnetic-permeability relaxation in this material.

II. EXPERIMENTAL

The $Fe_{73.5}Cu_1Nb_3Si_{13.5}B_9$ (at. %) ribbons were produced by melt spinning in air (supplied by IEN "Galileo Ferraris," Torino, Italy). Different sets of samples taken from the same ribbon were submitted to isothermal annealings at 540 °C and/or 550 °C for different times t_a(t_a=10, 20, 40, and 60 min). Transient temperature effects were minimized by rapidly inserting the sample in a large furnace of high heat capacity. The heat treatments were performed in Ar atmosphere. The samples were rapidly extracted from the furnace and left to cool at room temperature.

Mössbauer spectra were measured at room temperature in the transmission mode, using a conventional constant-acceleration setup with a Rh(^{57}Co) source.

The magnetostriction constant was measured using the small angle magnetization rotation (SAMR)[9] method. The magnetic disaccommodation was measured by a feedback technique keeping the magnetic induction constant.[10] The driving field variation $\Delta H=H(t_2)-H(t_1)$ between the fixed times $t_1=0.025$ s and $t_2=0.8$ s, after a domain-wall rearrangement, was measured as a function of the induction B for different annealing times;[4] the maximum value in the ΔH vs B curves was considered in order to compare the results obtained.[11] All measurements were performed at room temperature.

 0021-8979/92/126008-05$04.00

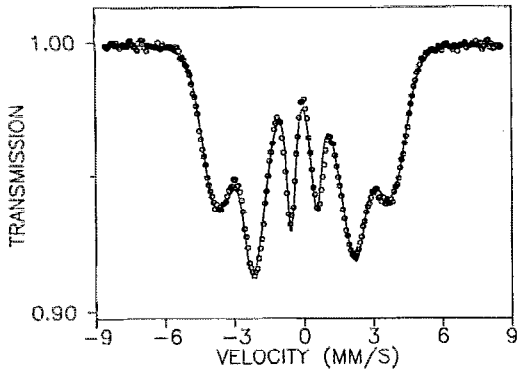

FIG. 1. Mössbauer spectrum of as-quenched $Fe_{73.5}Cu_1Nb_3Si_{13.5}B_9$ ribbon, fitted with the B_{hf} distribution of Eq. (1).

III. RESULTS AND DISCUSSION

A. Mössbauer spectroscopy

Figure 1 shows the spectrum of an as-quenched ribbon. Similar to most ferromagnetic metallic glasses, it shows broad magnetically split lines arising from a hyperfine field distribution. It was found that a good fit could be obtained with a "skew gaussian" distribution function

$$P(B)=\exp\left(-\frac{(B-B_0)^2}{2\sigma_i^2}\right), \qquad (1)$$

where $\sigma_i=\sigma_1$, σ_2 for $B<B_0$, $B>B_0$, respectively; a linear correlation between B_{hf} and isomer shift was included in order to account for the slight asymmetry of this spectrum.

Spectra of heat-treated samples exhibit a gradually developing structure, as can be seen in Fig. 2. These spectra were fitted with a superposition of five discrete magnetic sites and a continuous $P(B_{hf})$ of the form (1) above. Equal linewidths (0.32–0.36 mm/s) were assumed for all sites. Sextet line intensity ratios were left free to vary; I_3/I_1 was always close to 0.34, while $I_2/I_1\simeq 1.1$, indicating a near in-plane magnetic texture (the only exception was the unannealed sample, for which $I_2/I_1=0.73$, which is closer to, though larger than, the 2/3 ratio typical of a randomly distributed magnetization). Fitted parameters pertinent to the continuous field distributions and to the discrete spectra are reported in Tables I and II, respectively.

It can be appreciated from Fig. 2 that a large proportion of the alloy remains in the amorphous state after a standard heat treatment. The fraction of Fe nuclei in amorphous regions is given in Table I. The data further indicate a shift of $P(B_{hf})$ toward lower fields, reflecting the change in chemical composition of the amorphous phase as Fe and Si diffuse into crystalline regions.

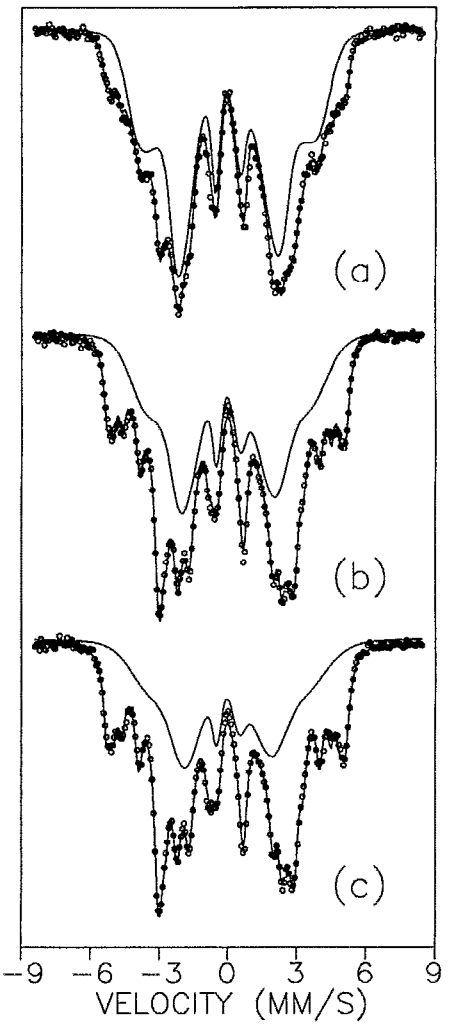

FIG. 2. Mössbauer spectra of annealed $Fe_{73.5}Cu_1Nb_3Si_{13.5}B_9$ samples: (a) 10 min at 540 °C, (b) 20 min at 540 °C, (c) 60 min at 550 °C, fitted as described in text. Inner curve shows the contribution from the amorphous component.

The B_{hf} values found for sites I–V (see Table II) are very similar to those reported for crystalline Fe-Si alloys in the 10–25% Si range. Such alloys are easily ordered with the DO_3 (Fe_3Al-type) structure. It has been shown[12,13] that the various B_{hf} can be assigned to Fe atom environments with different Fe nearest-neighbor (nn) numbers. Thus, subspectra III, IV, and V correspond to sites with 6,

TABLE I. Fitted values of the most probable hyperfine field B_0, low-field and high-field gaussian widths σ_1, σ_2, average field $B_{av}=\int BP(B)dB$, and relative absorption area of the amorphous component in Mössbauer spectra.

Treatment	As-cast	540 °C/10′	540 °C/20′	540 °C/40′	550 °C/60′
B_0(T)	24.0	24.1	21.7	22.6	19.9
σ_1(T)	6.4	7.2	7.5	8.1	7.8
σ_2(T)	2.9	2.8	4.5	4.0	5.7
B_{av}(T)	21.2	20.6	19.3	19.3	18.2
%	100.0	77.8	57.9	57.3	45.8

TABLE II. Fitted hyperfine fields (T) and relative populations of crystalline sites in Mössbauer spectra.

Treatment	540 °C/10′		540 °C/20′		540 °C/40′		550 °C/60′	
sites	B_{hf}	%	B_{hf}	%	B_{hf}	%	B_{hf}	%
I	32.6	22.7	32.3	23.2	32.2	24.0	32.3	24.2
II	31.0	26.1	30.7	21.1	30.7	19.4	30.6	18.1
III	28.7	21.1	28.3	17.9	28.3	17.2	28.3	16.7
IV	24.1	13.2	24.4	19.6	24.4	20.5	24.5	22.1
V	19.3	17.1	19.5	18.2	19.5	18.9	19.5	18.8

5, and 4 nn Fe (A_6, A_5, and A_4). Subspectra I and II, on the other hand, belong to sites with 7(A_7) and 8(A_8 and D) nn Fe, but there is an ambiguity regarding the B_{hf} at the D site.[12,13]

The general agreement (within better than 1%) with published B_{hf} data is strong evidence that the crystalline phase formed is pure Fe-Si solid solution; small amounts of dissolved B would be expected to reduce the B_{hf}'s measurably. This result rules out the speculation[2,14] that some B could be dissolved in the Fe-Si phase. An analogous conclusion has been drawn from lattice parameter considerations[7] and from atom probe analysis data.[15]

No Fe borides, such as reported by Zemčik *et al.*[16] and by Kohmoto *et al.*,[17] have been found in our samples.

The Si concentration in $Fe_{1-x}Si_x$ can be evaluated by comparing the relative intensities of subspectra I–V with the calculated fractional populations of the corresponding Fe environments for a Si-deficient DO_3 structure. These are given by

$$f(D)=\frac{1-2x}{2(1-x)} \tag{2}$$

for the D site (8 nn) and

$$f(A_n)=\frac{4!}{(n-4)!(8-n)!}\times\frac{(1-4x)^{n-4}(4x)^{8-n}}{2(1-x)} \tag{3}$$

for the A_n sites ($4\leqslant n\leqslant 8$). On account of the uncertain assignment of the D site, the added intensities of subspectra I and II were associated with the superposition of D, A_7, and A_8 sites. The best x for each sample was found by the least-squares method. The results, displayed in Fig. 3, show a rapid evolution from $x=15.5\%$ [i.e., the Si/(Fe+Si) ratio in the amorphous alloy] to the final value $x=(18.2\pm0.5)\%$ Si in the crystalline grains.

The volume fractions of amorphous and crystalline regions can be estimated from the corresponding absorption areas in the Mössbauer spectra, which give the relative proportion of Fe atoms in both regions. By combining the absorption percentage (Table I) with the Fe-Si composition results (Fig. 3), and taking into account the Si/Fe atomic volume ratio, we obtain the volume fractions shown in Table III. We note the 51% amorphous volume fraction obtained after a 1 h annealing at 550 °C is in very good agreement with the result obtained by Gawior and Woch[18] from x-ray diffraction.

It is noteworthy that the amorphous phase remaining after a 1 h treatment still contains an appreciable amount of Si. Indeed, if only Fe and Si atoms are assumed to migrate into crystalline regions, the composition of the amorphous phase can be estimated to be $Fe_{65.5}Cu_{1.9}Nb_{5.8}Si_{9.4}B_{17.4}$.

B. Magnetostriction and disaccommodation

Figure 4 shows the evolution of the saturation magnetostriction for different thermal treatments with increasing times. This behavior is explained from the balance in the magnetostriction ($\lambda_S^{\rm tot}$) among the crystalline grains and the residual amorphous matrix:[3]

$$\lambda_S^{\rm tot}=\nu_{\rm cr}\lambda_S^{\rm cr}+(1-\nu_{\rm cr})\lambda_S^{\rm am}, \tag{4}$$

where $\nu_{\rm cr}$ denotes the volume fraction of the α-FeSi phase. Using the magnetostriction results in addition to the volume fraction estimated from Mössbauer experiments (see Table III), it is possible to estimate the magnetostriction of the amorphous phase as a function of annealing time. For this purpose, values of magnetostriction for polycrystalline α-FeSi were interpolated and calculated from published data.[19] The results obtained are shown in Table III and are also plotted in Fig. 4. This result clearly illustrates the high sensitivity of the magnetostriction constant to the structural and compositional changes occurring during the development of the nanocrystalline state.

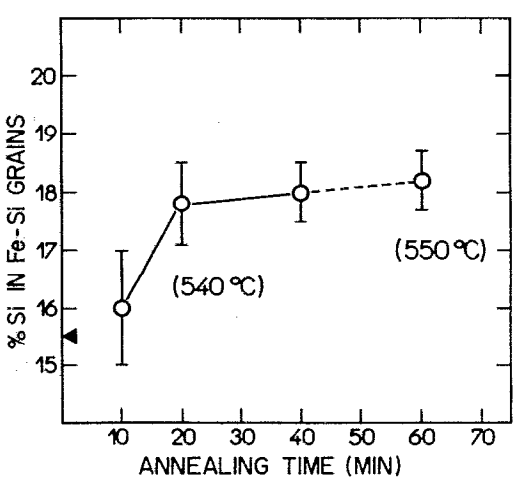

FIG. 3. Si concentration (at. %) in Fe-Si nanocrystals as a function of annealing time. Arrowhead indicates Si/(Fe+Si) ratio in as-quenched alloy.

TABLE III. Crystalline volume fraction estimated from Mössbauer results v_{cr}, measured magnetostriction λ_S^{tot}, crystalline Fe-Si magnetostriction λ_S^{cr} (from Ref. 19), calculated magnetostriction of amorphous phase λ_S^{am}, and magnetic disaccommodation ΔH.

Treatment	As-cast	540 °C/10′	540 °C/20′	540 °C/40′	550 °C/60′
v_{cr}	0	0.19	0.38	0.39	0.49
$\lambda_S^{tot}(10^{-6})$	22.3	13.5	7.36	3.16	2.0
$\lambda_S^{cr}(10^{-6})$	···	−2.5	−3.5	−3.6	−3.7
$\lambda_S^{am}(10^{-6})$	22.3	17.3	14.0	7.5	7.5
$\Delta H(10^{-3}$ A/m)	72	3	1	0.7	0.5

Using the magnetostriction values estimated above for the amorphous phase (λ_S^{am}), it is possible to verify the main sources of magnetic permeability relaxation in the nanocrystalline materials. According to the main theories proposed to explain the magnetic disaccommodation in amorphous alloys,[11,20,21] a quadratic relationship is expected to hold between the disaccommodation and saturation magnetostriction at a given temperature. In particular, for Fe-based amorphous alloys the Allia and Vinai model[11] predicts:

$$\Delta H = A N_T \lambda_S^2, \tag{5}$$

where N_T is the number of defects effective at temperature T, and A is a constant which includes several factors that are not modified by structural relaxation.

Since N_T changes during heat treatments, a reference sample was prepared by preannealing an amorphous ribbon for 1 h at 300 °C. This temperature is too low to initiate crystallization, so this treatment was intended to produce a state in which nearly all irreversible processes had occurred, i.e., a state with greatly relaxed internal stresses and homogenized free volume distribution. The measured disaccommodation for this sample was $\Delta H = 35 \times 10^{-3}$ A/m, which is a factor of 2 smaller than for an as-cast sample. This effect can be explained by assuming changes in two-level system parameters, such as a reduction of their total number N_T and/or a change in energy splitting.[20]

Figure 5 shows the results of magnetic disaccommodation versus the square of the estimated λ_S for the amorphous phase. Already after 10 min annealing at 540 °C, a very strong reduction in the disaccommodation value is observed. Simply, the very low disaccommodation values in nanocrystalline materials could be interpreted as an effect of the high reduction of amorphous volume which, in turn, suffered a strong structural relaxation combined with a reduction in λ_S^{am}. However, it is clearly verified that the quadratic behavior is not followed (Fig. 5, dashed curve), even if the relaxed sample is taken as the initial point (Fig. 5, dotted curve). In this way, the almost complete suppression of magnetic disaccommodation in nanocrystalline $Fe_{73.5}Cu_1Nb_3Si_{13.5}B_9$ can only be explained by either the annihilation or freezing of most of the structural defects responsible for this time effect, in agreement with the ideas proposed by Allia *et al.*[4]

IV. CONCLUSIONS

We have used Mössbauer spectroscopy to study the development of a nanocrystalline structure in an amorphous $Fe_{73.5}Cu_1Nb_3Si_{13.5}B_9$ alloy for different annealing times. Both the composition and volume fraction of the crystalline grains could be quantitatively determined. After a standard 1 h heat treatment at 550 °C, an ordered $Fe_{82}Si_{18}$ alloy was obtained, with no indication of any other

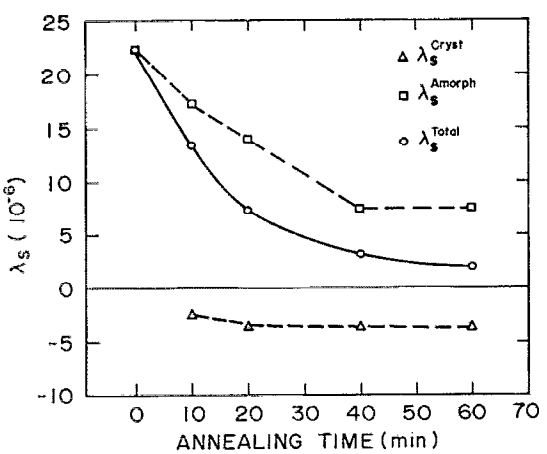

FIG. 4. Saturation magnetostriction as a function of annealing time: λ_S^{tot}(measured), λ_S^{cr}(from Ref. 19), and λ_S^{am}[calculated with Eq. (4)].

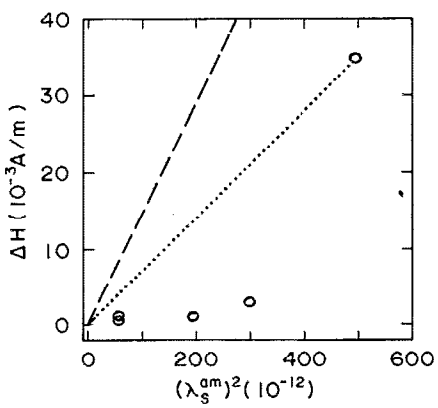

FIG. 5. Driving field variation ΔH (see Ref. 4) as a function of amorphous saturation magnetostriction squared. Dashed and dotted curves represent the expected quadratic behavior considering, respectively, the as-cast sample and the preannealed sample data as starting points.

crystalline phases. For shorter annealing times, our results suggest a gradual Si enrichment of the Fe-Si phase, though the transformation appears to be essentially complete after 20 min.

The volume fraction of the retained amorphous phase $\sim 50\%$, is larger than early estimates, but agrees well with recent x-ray determinations for similarly treated alloys. The discrepancies concerning volume fractions obtained by different authors (e.g., Ref. 22) might be related to differences in the initial amorphous state of the samples, as well as different heating and cooling rates.[23]

By combining the Mössbauer data with magnetostriction results it has been possible to evaluate the time evolution of the crystalline phase contribution to the total measured magnetostriction, and thus to estimate the contribution of amorphous regions. In addition, using the extremely sensitive experimental technique of magnetic disaccommodation, it has been verified that the development of the nanocrystalline state has great influence on the degree of freedom of local defects inherent to the amorphous structure.

ACKNOWLEDGMENTS

We are indebted to Dr. F. Vinai for supplying samples, to Dr. R. Grössinger and Dr. W. Gawior for helpful discussions, and to Dr. G. Herzer for help with crystalline magnetostriction data. This work was financially supported by FAPESP and CNPq/RHAE.

[1] H. Gleiter, Prog. Mater. Sci. **33**, 223 (1989).
[2] Y. Yoshizawa, S. Oguma, and K. Yamauchi, J. Appl. Phys. **64**, 6044 (1988).
[3] G. Herzer, paper presented at Soft Magnetic Materials 10 Conference, Dresden, (Sept. 1991), to be published in J. Magn. Magn. Mater.
[4] P. Allia, C. Beatrice, F. Vinai, M. Knobel, and R. Sato Turtelli, Appl. Phys. Lett. **59**, 2454 (1991).
[5] G. Herzer, IEEE Trans. Magn. **MAG-26**, 1397 (1990).
[6] Y. Yoshizawa and K. Yamauchi, Mater. Trans. JIM **31**, 307 (1990).
[7] U. Köster, U. Schünemann, M. Blank-Bewersdorf, S. Brauer, M. Sutton, and G. B. Stephenson, Mater. Sci. Eng. A **133**, 611 (1991).
[8] Y. Yoshizawa and K. Yamauchi, Mater. Sci. Eng. A **133**, 176 (1991).
[9] K. Narita, I. Yamasaki, and H. Fukunaga, IEEE Trans. Magn. **MAG-16**, 435 (1980).
[10] P. Allia, C. Beatrice, G. Brida, and F. Vinai, J. Magn. Magn. Mater. **101**, 49 (1991).
[11] P. Allia and F. Vinai, Phys. Rev. B **26**, 6141 (1982).
[12] M. B. Stearns, Phys. Rev. **129**, 1136 (1963).
[13] L. Häggström, L. Gränäs, R. Wäppling, and S. Devanarayanan, Phys. Scripta **7**, 125 (1973).
[14] M. Fujinami, Y. Hashiguchi, and T. Yamamoto, Jpn. J. Appl. Phys. **29**, L477 (1990).
[15] K. Hono, A. Inoue, and T. Sakurai, Appl. Phys. Lett. **58**, 2180 (1991).
[16] T. Zemčik, Y. Jirásková, K. Záveta, D. Eckert, J. Schneider, N. Mattern, and D. Hesske, Mater. Lett. **10**, 313 (1991).
[17] O. Kohmoto, K. Haneda, and T. Choh, Jpn. J. Appl. Phys. **29**, L1460 (1991).
[18] W. Gawior and M. Woch, J. Magn. Magn. Mater. (in press).
[19] T. Yamamoto, *The Development of Sendust and Other Ferromagnetic Alloys* (Komiyama Printing, Chiba, Japan, 1991), p. 26.
[20] P. Allia and F. Vinai, Phys. Rev. B **33**, 422 (1986).
[21] H. Kronmüller, N. Moser, and F. Rettenmeier, IEEE Trans. Magn. **MAG-20**, 1388 (1984).
[22] G. Herzer, IEEE Trans. Magn. **MAG-25**, 3327 (1989).
[23] R. Grössinger, C. Polak, M. Knobel, and R. Sato Turtelli (unpublished).